ISIJ International, Vol. 36 (1996), Supplement, pp. S163–S166

Simulation of Shell Strength Properties by the SSCT Test

Christian BERNHARD, Herbert HIEBLER and Manfred M. WOLF[1)]

Department of Ferrous Metallurgy, Montanuniversität, A-8700 Leoben, Austria.
1) Wolftechnology, CH-8032 Zürich, Switzerland.

(*Received on April 16, 1996; accepted in final form on July 15, 1996*)

Initial shell formation and surface quality in continuous casting are affected by thermal and mechanical stresses which may lead to crack formation during solidification. Thus, detailed knowledge of high temperature strength properties as function of steel composition is required under given conditions. To simulate shell straining by tensile force perpendicular to the main dendrite growth axis, the "Submerged Split Chill Tensile" (SSCT) test was (and still is) further developed. The present report details updated results for ferritic and austenitic iron, and compares different chill materials. The determined effect of P-content on shell strength is quantified. Primary dendrite arm spacing without and with load appears to indicate that tensile elongation is not uniformly distributed over the test length.

KEY WORDS: continuous casting; strand surface quality; solidification cracking; *in situ* tensile test; high temperature strength and elongation; P-microsegregation; primary dendrite arm spacing.

1. Introduction

Defect-free surface quality in continuous casting requires the prevention of crack formation during initial solidification and shell growth.[1)] Hence, it is important to determine the mechanical properties of steel under conditions closely simulating initial shell formation and the respective loading conditions:

- high cooling rates of 10^1–10^3 K/s to simulate the fine (cellular) dendritic microstructure, and the corresponding microsegregation behavior near the strand surface;
- a non-isothermal temperature distribution with a temperature gradient comparable to the strand shell in the mold;
- tensile loading at a low strain rate of about 0.0005–0.005/s, and perpendicular to the main dendrite growth direction to initiate interdendritic ("intercolumnar") crack formation during shell growth.

These simulation requirements are closely met by the new SSCT- (Submerged Split Chill Tensile) test, initially developed for aluminum and Al-alloys[2)] then, progressively applied to steels[3–5)]—with a total of about 200 tests to date. The present work reports the most recent results on low and high C-steels, and varying the P-content.

2. Experimental

In the SSCT-test a cylindrical chill body, split in two halves and composed of either copper (water-cooled) or steel (without inner cooling) is submerged into liquid steel and held for a few seconds until a coherent steel is formed (**Fig. 1**). Then, the lower half is moved by a hydraulic ram downward to strain the solid shell during its growth. For heat flux control, the chill surface is coated with alumina of varying thickness (such coating also facilitating the shell removal from the chill after testing).

During the entire test, the heat flux is derived from immersed thermocouples (compare Fig. 1, item 4) and converted into shell growth, solid fraction and temperature gradient by computer calculation. The numerical procedure includes a microsegregation model to define the actual solid shell portion. **Figure 2** illustrates this procedure for an extra-low C-steel (0.018% C). T_b is the so-called bulk temperature and characterizes the average shell temperature, in this example close to 1 400°C at about 4 mm shell thickness. Also shown is the locus of the delta-to-gamma transformation of this hypoperitectic steel.

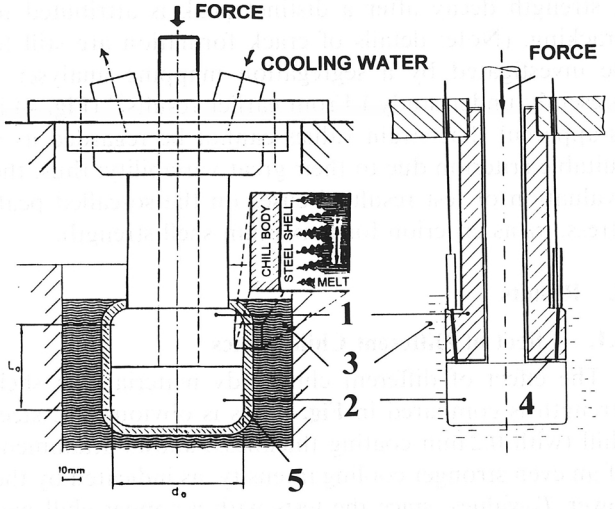

Fig. 1. Two types of chill bodies used in SSCT test (1 = upper half; 2 = lower half; 3 = liquid steel bath; 4 = thermocouple; 5 = solid steel shell).

© 1996 ISIJ

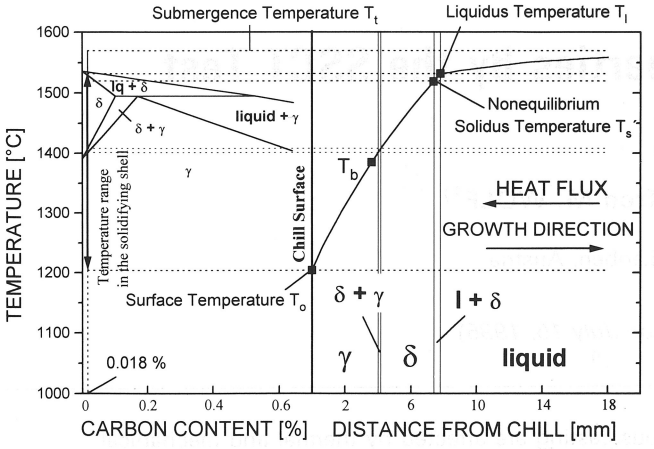

Fig. 2. Example of thermal analysis during SSCT-test for 0.018 % C-steel.

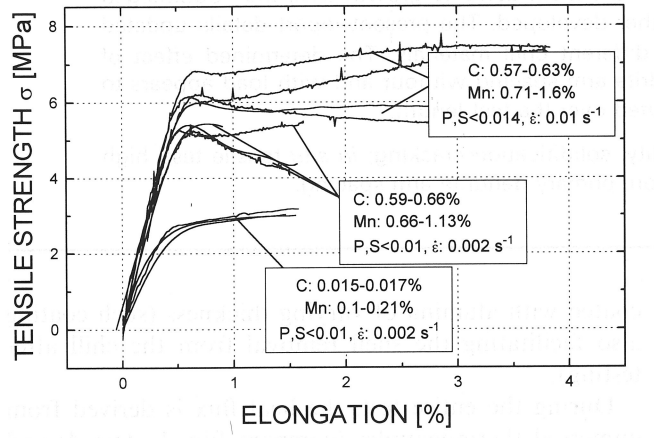

Fig. 3. Strength–elongation curves for low and high C-steels in the SSCT-test.

The characteristic strength–elongation curves obtained in the SSCT-test are exemplified for low and high C-steels in **Fig. 3**, which clearly attests to the excellent test reproducibility by the similar shape of curves for similar steel grades. Also, the difference between various strain rates complies with the expected trend.

For the given measuring length of 50 mm and a maximum uniform elongation of 4 %, it is assumed that no cracks are formed in curves with a plateau, whereas a strength decay after a distinct peak is attributed to cracking. (Note: details of crack formation are still to be investigated by a segregation mapping analyser—presently under study.) From earlier results[5] (**Fig. 4**) it is apparent that strain values cannot be regarded as a suitable criterion due to their great variability; thus, the evaluation of test results focuses on the so-called peak stress, σ_P as criterion for maximum shell strength.

3. Results

3.1. Effect of Different Chill Bodies

The effect of different chill body materials on shell strength is compared in **Fig. 5**. As is obvious, the steel chill (with 0.2 mm coating thickness) allows attainment of an even stronger cooling intensity, as indicated by the lower T_b-values, since the tests with a copper chill had been conducted in an earlier series with rather thick alumina coating of 0.5 mm.[3]

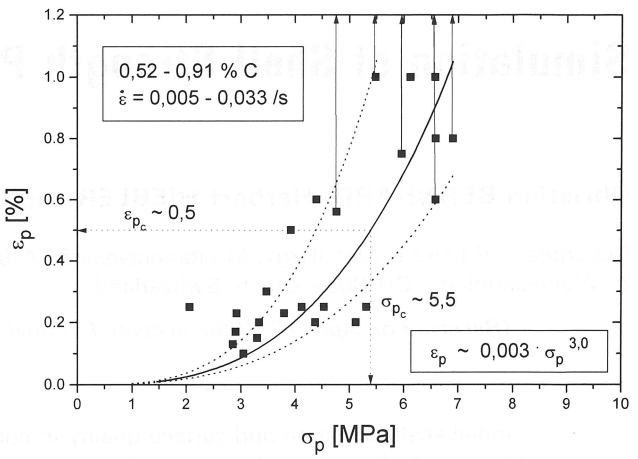

Fig. 4. Strain (at peak stress) *vs.* peak stress in SSCT-test for high C-steels.[5]

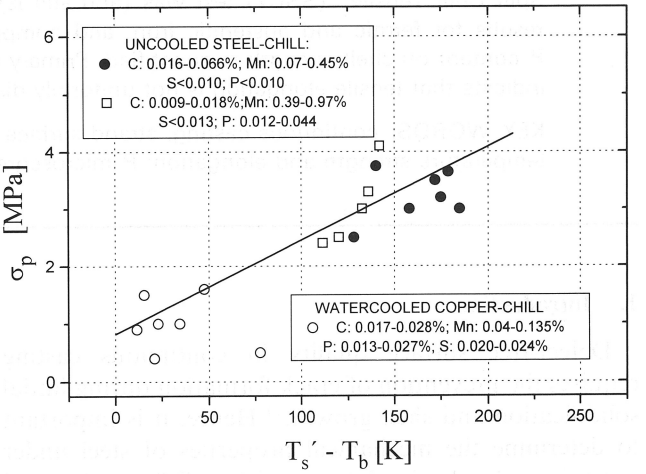

Fig. 5. Strength increase with temperature below solidus for extra-low C-steels and two chill bodies, the copper chill tests from.[3]

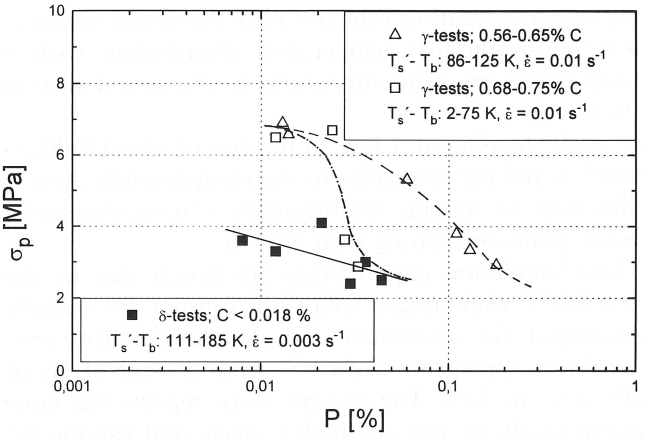

Fig. 6. Effect of P-content on maximum shell strength for ferritic and austenitic iron in the SSCT-test.

3.2. Effect of P-content

Test results as a function of P-content are plotted for low and high C-steels in **Fig. 6**; the high C-series is distinguished by thin and thick shells (as expressed by the T_b-value). The former show a sudden drop in strength down to the level of ferritic iron which points to a complex interaction with the P-content, presumably connected with a eutectic Fe_3P–Fe_3C formation.[6]

© 1996 ISIJ

4. Discussion

4.1. Crack Criterion

A strain criterion is usually applied in caster design as well as in process optimisation.[5] However, it has been suspected for some time that tensile elongation at the solid/liquid interface is not uniformly distributed but, rather, is concentrated at "weak" spots between dendrites, *e.g.*, with a positive growth angle between two neighboring stems; hence, crack initiation is actually caused by a much larger than average strain[7] (**Fig. 7**). Such process of strain "accumulation" over solidification time has been investigated more recently in hot tensile tests (load applied parallel to the dendrite growth axis) by Yamanaka *et al.*,[8] and the "brittle" temperature range of crack extension determined by the solid fraction $f_S = 0.80$–0.99; this criterion was also used in the present work.

To investigate the effect of tensile load on primary dendrite arm spacing, measurements without and with load were made for samples (with crack, see arrow) located near the gap between the two chill halves, *i.e.*, midway in test length (**Fig. 8**). As observed, the spacing increase of about 10% is significantly larger than the maximum uniform elongation of 4%. This could indicate that this cracked shell portion has indeed been strained much more heavily than the rest of the material. More investigations into this aspect are planned.

4.2. P-effect

Compared to S-effects, relatively little is yet known about interdendritic P-segregation and its effects on crack formation. In hot tensile tests at a high strain rate of 5/s (again, with load axis parallel to dendrite growth), Suzuki *et al.*[9] observed a strong ductility decrease (reduction of area) with increasing P-content for high C-steels, but little P-effect below 0.25% C. Even for high C-steel, high ductility was found at a low strain rate of about 0.001/s. This improvement was attributed to the reduction of metastable phosphides of type $(FeMn)_3P$ accumulated along austenite grain boundaries during cooling.

In contrast, the present results of Fig. 6 not only yield embrittlement phenomena for high C-steels but for low C-steels too, and at the low strain rates applied. Hence, the load application in the SSCT-test (as in the real strand shell) perpendicular to the main dendrite growth axis appears to be much more sensitive to interdendritic (and intergranular) segregation effects. These results also confirm that shell strength data are indeed a suitable criterion to define steel composition dependent crack susceptibility.

As indicated above, detailed investigations are planned on interdendritic segregation by using a concentration mapping analyser in the near future.

4.3. Strength Data

As in earlier reports on SSCT-tests,[3–5] the present findings are compared with pertinent literature data[10–12] of similar strain rate (**Fig. 9**). Again, all SSCT-data can be correlated with the same slope of strength *vs.* test temperature as derived previously,[5]

$$\sigma_p = \sigma_m \exp \beta(1 - T_b/T_m) \quad \text{.....(1)}$$

with $\beta = 7$.

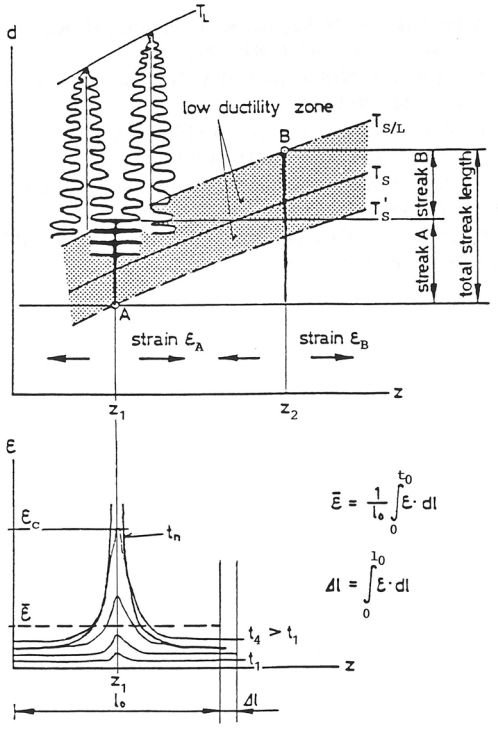

Fig. 7. Schematic of shell growth over time, and of crack formation in the "brittle" temperature range due to interdendritic strain concentration during tensile loading, from.[7]

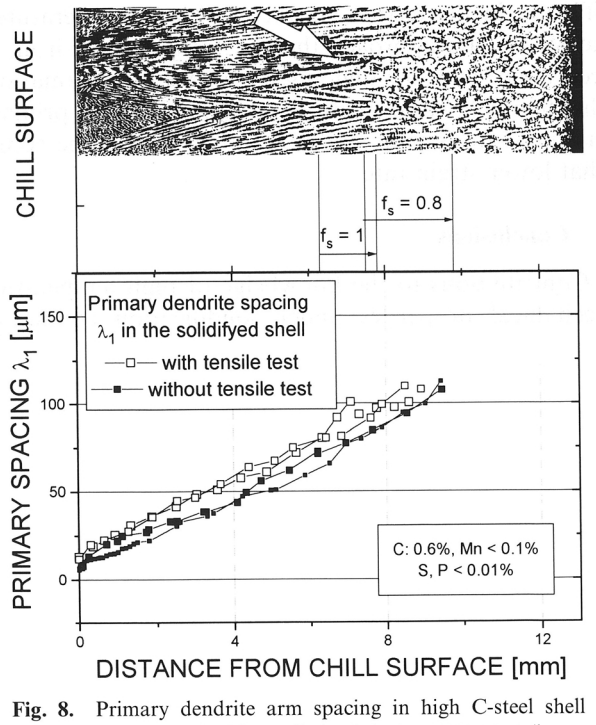

Fig. 8. Primary dendrite arm spacing in high C-steel shell without and with tensile load during SSCT-test (lower graph), and etched shell cross section (Oberhoffer's reagent) showing crack location (indicated by the arrow) and concurrent displacement of the critical isotherms of $f_S = 0.8$ and 1.0 respectively during the tensile test (upper photo) *vs.* distance from chill surface.

© 1996 ISIJ

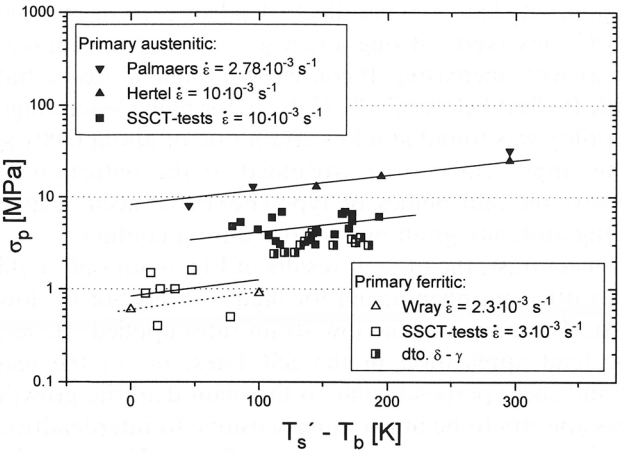

Fig. 9. Strength increase over temperature below solidus in the SSCT-test for ferritic and austenitic iron compared with literature data.[10–12]

However, while the literature data yield a hypothetical strength at melting point T_m of $\sigma_m = 8$ MPa for austenitic iron, the SSCT-data average a value of $\sigma_m = 3$ MPa only, this significant discrepancy attributed to the greater sensitivity to interdendritic (and intergranular) segregation effects in case of shell loading perpendicular to the dendrite growth axis. (Note: in some hot tensile tests, partially radial dendrite growth was attempted by inert gas cooling of the sample from the side during testing.[12,13])

For ferritic iron, very close agreement with the data by Wray[10] is obtained above the A_{r4}-temperature, *i.e.*, $\sigma_m = 0.6$ and 0.8 MPa, respectively, which indicates little sensitivity to structural effects on account of high back diffusion in the ferritic matrix. At lower temperatures, the SSCT-data approach the level of austenitic iron, in accordance with the ongoing δ–γ phase transformation. The slightly lower strength level, compared with primary austenitic steels, may again be attributed to the somewhat lower strain rate.

5. Conclusions

Contributions to the knowledge of high temperature mechanical properties under solidification conditions were made by closely simulating initial shell formation and growth in the continuous casting mold in further work with the new SSCT-test, with the following results.

(1) Good test reproducibility was again verified by the close similarity of strength–elongation curves when testing similar extra-low as well as high C-steels.

(2) Tensile strain does not seem to be a suitable criterion for crack formation due to apparently localised strain concentration at preferred interdendritic sites.

(3) Peak stress, on the other hand, allows reliable determination of the near-solidus creep resistance at low strain rates typical of strand shell deformation, and also yields a useful criterion for steel composition dependent crack susceptibility, as illustrated for the case of P-content in both ferritic and austenitic iron.

Acknowledgments

Primary dendrite arm spacing measurements by G. Wieser, and microscopy work by S. Schider are gratefully acknowledged.

REFERENCES

1) M. M. Wolf: On the Relationship between Initial Solidification and Strand Surface Condition of Peritectic Steels, Habilitation-Thesis, submitted to Montanuniversität, Leoben/Austria, (1996).
2) P. Ackermann, W. Kurz and W. Heinemann: *Mater. Sci. Eng.*, **75** (1985), 79.
3) G. Xia, J. Zirngast, H. Hiebler and M. M. Wolf: Proc. Conf. Cont. Casting of Steels in Developing Countries, The Chinese Soc. for Met., Beijing, (1993), 200.
4) H. Hiebler and M. M. Wolf: *CAMP-ISIJ*, **6** (1993), 1132.
5) H. Hiebler, J. Zirngast, C. Bernhard and M. M. Wolf: *Steelmaking Conf. Proc.*, **77** (1994), 405.
6) T. W. Clyne, M. M. Wolf and W. Kurz: *Metall. Trans. B*, **13B** (1982), 259.
7) A. Vaterlaus and M. Mangin: *Steelmaking Conf. Proc.*, **68** (1985), 471.
8) A. Yamanaka, K. Nakajima, K. Yasumoto, H. Kawashima and K. Nakai: *Rev. Mét.-CIT*, **89** (1992), 627.
9) H. G. Suzuki, S. Nishimura and Y. Nakamura: *Trans. Iron Steel Inst. Jpn.*, **24** (1984), 54.
10) P. J. Wray: *Metall. Trans. A*, **7A** (1976), 1621.
11) A. Palmaers: *Met. Rep. CRM*, (1978), No. 53, 23.
12) J. Hertel, H. Litterscheidt, U. Lotter and H. Pircher: *Rev. Mét.-CIT*, **89** (1992), 73.
13) P. R. Scheller, P. Papaiacovou, D.-Y. Lin, M. Cöl and W. Dahl: *Steel Res.*, **66** (1995), 530.

© 1996 ISIJ